RELATIONSHIP OF HEAVY PRECIPITATION TO THE JET MAXIMUM IN THE EASTERN UNITED STATES, SEPTEMBER 19–21, 1958

DONALD A. RICHTER AND ROY A. DAHL

National Weather Analysis Center, U. S. Weather Bureau, Washington, D. C.

1. INTRODUCTION

During September 19–21, 1958, precipitation, which had been occurring in rather large amounts over the western Gulf States, began spreading northeastward through the Ohio River Valley without benefit of any marked surface cyclogenesis. This paper analyzes the relationship between the rainfall pattern and the progression of wind maxima along the jet.

In addition, the paper investigates a semi-objective method for 24-hour quantitative precipitation forecasting using vertical motion charts of the Joint Numerical Weather Prediction (JNWP) Unit. This method of quantitative precipitation forecasting was developed on an experimental basis by Gilman et al. [1] and has been adopted by the National Weather Analysis Center (NAWAC) with some modifications aimed at reducing the time consumed in lengthy computation.

2. SYNOPTIC SITUATION

At the surface at 1200 GMT, September 19, 1958 (fig. 1A), a fairly large ridge extended from eastern Canada south-southwestward to the Central States and a weak stationary front stretched across the northern Gulf of Mexico. Another very weak and diffuse stationary front extending north-south through the Plains States was subsequently frontolized because of lack of thermal support (note superimposed thickness lines). Meanwhile, a strong maritime polar front had entered the Pacific Northwest.

At 500 mb. (fig. 1B), a ridge lay over the Ohio Valley in a position similar to that of the surface High and a trough extended from the Dakotas southward through New Mexico. Farther west a pronounced short-wave trough accompanying the surface system was located just off the west coast.

Twelve hours later (fig. 2B), the western trough had progressed inland to the Rocky Mountains. The height rises induced in the ridge ahead of this trough had caused the trough previously located over the Plains States to fill and move eastward more rapidly in the northern portion, thus to shear off from the southern portion of the trough. A weak Low appeared to be forming just east of Amarillo, Tex., and the downstream ridge moved eastward over the Appalachian Mountains.

At the surface (fig. 2A) a poorly defined area of cyclogenesis appeared in eastern Texas in conjunction with the cutoff 500-mb. Low forming near Amarillo.[1] A general katabaric area of 4 mb. per 12 hours covered the entire Mississippi Valley as the ridge of high pressure moved toward the Atlantic coast; larger pressure falls occurred in the Northern Plains States ahead of the approaching maritime polar system.

At 1200 GMT, September 20 (fig. 3A), the diffuse Low in the Gulf States which had moved rather slowly during the preceding 12 hours was near the Louisiana-Texas border, and the High lay over the east coast. Meanwhile, the maritime polar system in western United States had been steadily advancing eastward and was situated in the eastern Dakotas.

Concurrently, the westernmost trough at 500 mb. (fig. 3B) had progressed east of the Continental Divide and a more definite Low in association with the surface system in the Lower Mississippi Valley region had appeared in southwestern Missouri.

By 0000 GMT, September 21 (fig. 4A), the Gulf States surface Low had moved quite rapidly and become better defined over Kentucky, even though very little deepening had occurred possibly due to the absence of thermal advection. The ridge to the east was now off the Atlantic coast and the advancing maritime polar front was steadily narrowing the distance between itself and the Low in Kentucky.

The associated trough and Low at 500 mb. (fig. 4B) had been forced to accelerate northeastward to a position just south of Lake Michigan as a result of the more vigorous and relatively fast-moving trough now over the Northern and Central Plains States. Twelve hours later, at 1200 GMT, September 21 (fig. 5B), all that remained of the first short-wave trough was a minor indentation over Lake Erie in the general circulation of the more pronounced trough over the Minnesota-Iowa area.

The conditions that existed at the 500-mb. level were reflected at the surface (fig. 5A). The Low near Pittsburgh, Pa., had deepened several millibars, and was moving northward toward the region of falling pressures preceding the maritime polar system approaching from the west. Subsequent maps at both the surface and 500 mb.

[1] If the remnant of tropical storm Gerda [2], which had weakened from a closed circulation to an easterly wave near Jamaica 4 days earlier, had moved at approximately the speed indicated by continuity, its location near eastern Texas at this time conceivably could have been the triggering device for cyclogenesis. However, lack of surface ship reports in the Gulf of Mexico and the diffuse character of the easterly wave made tracking the storm from chart to chart extremely difficult.

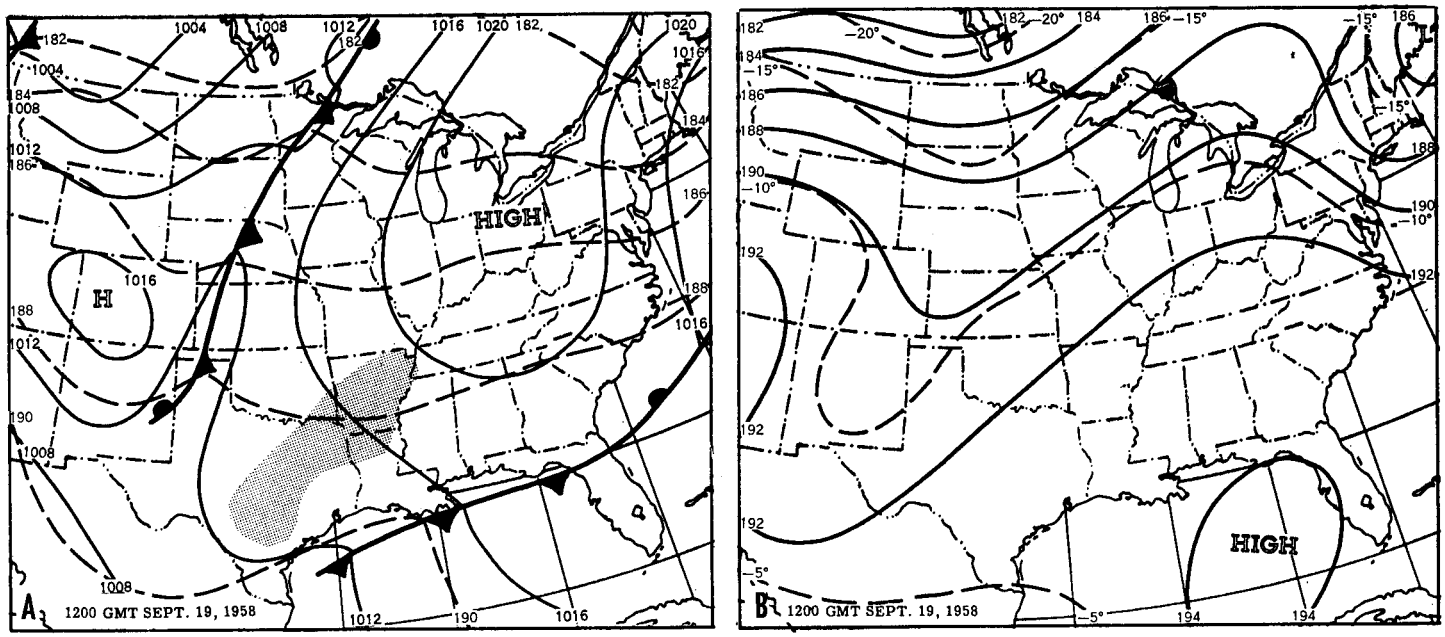

FIGURE 1.—1200 GMT, September 19, 1958. (A) Surface synoptic chart with superimposed 1,000–500-mb. thickness lines (dashed) in hundreds of geopotential feet. Shaded areas correspond to current precipitation. (B) 500-mb. contours (solid lines in intervals of 200 geopotential feet) and isotherms (dashed lines in ° C.).

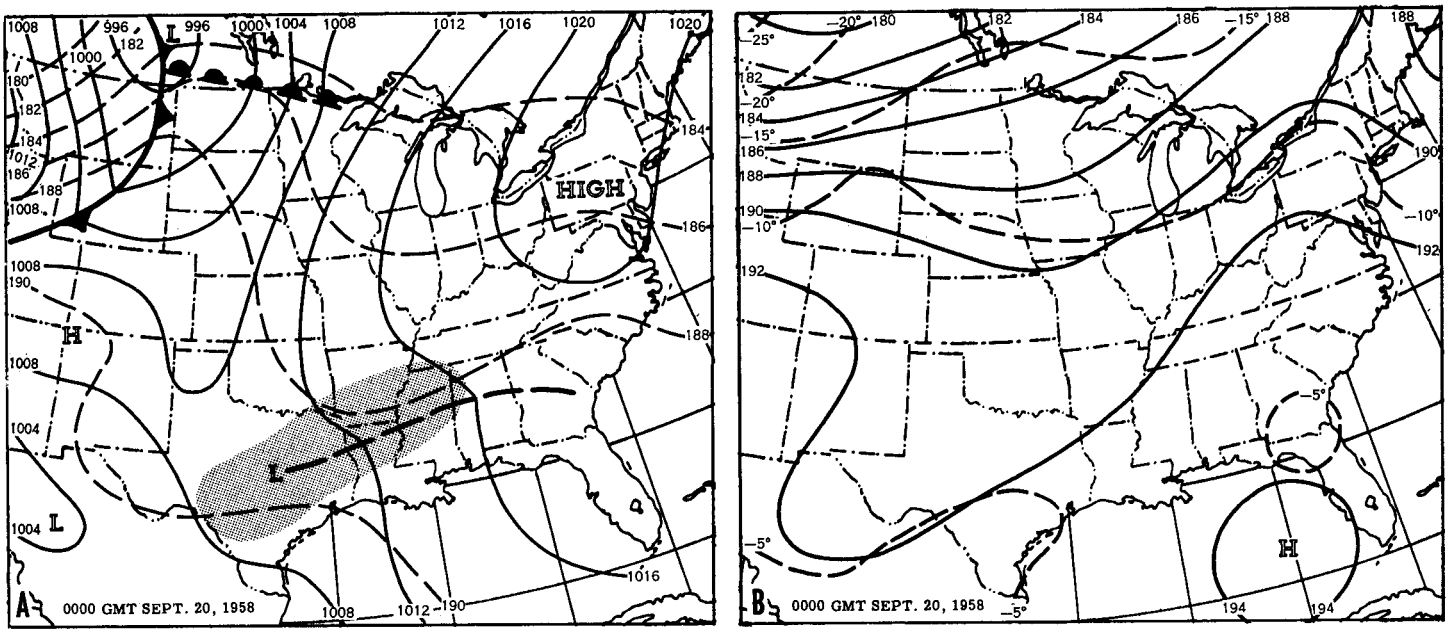

FIGURE 2.—Surface and 500-mb. charts for 0000 GMT, September 20, 1958.

(not shown) revealed that this small cyclone was eventually absorbed into the more dominant, larger-scale circulation. It is noteworthy how much stronger was the thermal advection associated with the maritime polar front in the Northern Plains States than the thermal advection of the weaker low pressure system.

3. RELATIONSHIP OF PRECIPITATION TO ADVECTION OF RELATIVE VORTICITY

In this section, we briefly summarize some relationships between vorticity advection and precipitation areas, based on a study by Riehl et al. [3]. These relationships, which will serve in section 4 as a basis for discussing effects of the jet stream on precipitation, are:

1. Advection of cyclonic vorticity, that is, flow across the gradient of vorticity from regions of greater to lesser cyclonic relative vorticity, results in divergence aloft which leads to upward vertical motion, a necessary condition for pressure falls and/or precipitation.

2. The vorticity distribution in a wave in the mid-troposphere zonal westerlies—cyclonic relative vorticity in the trough and anticyclonic relative vorticity on the

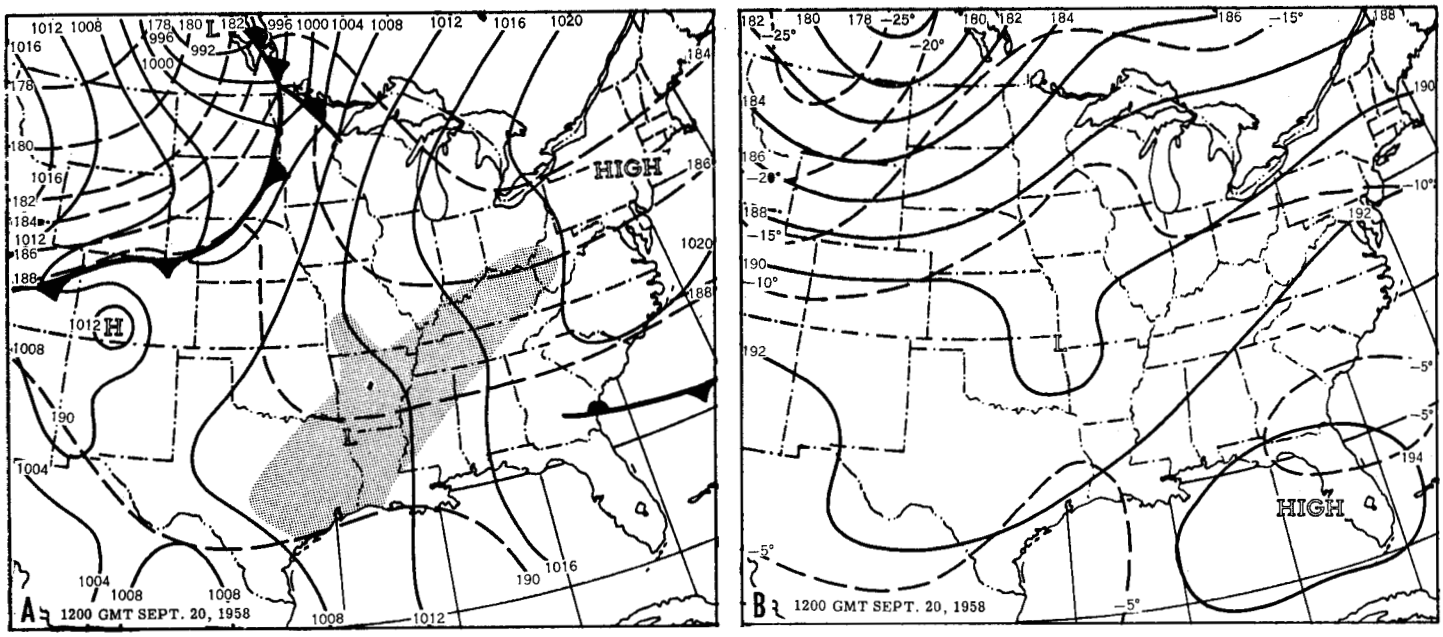

FIGURE 3.—Surface and 500-mb. charts for 1200 GMT, September 20, 1958.

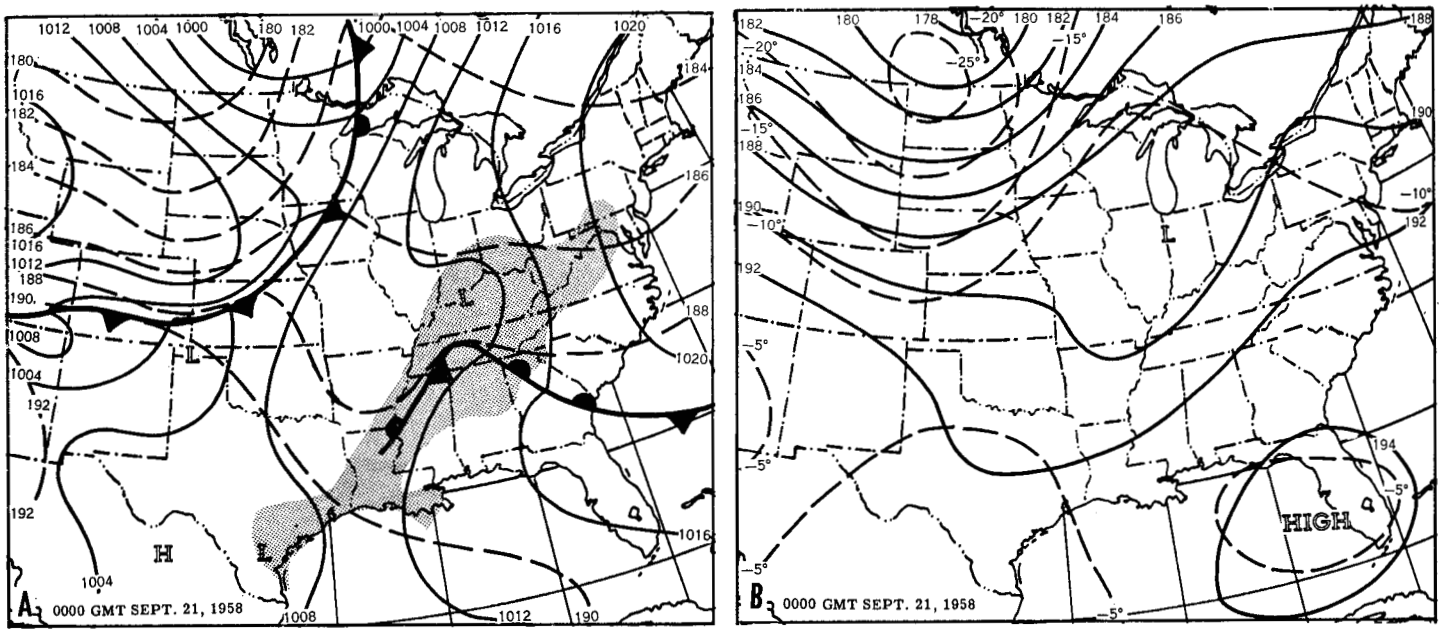

FIGURE 4.—Surface and 500-mb. charts for 0000 GMT, September 21, 1958.

ridge—makes the area between the trough and the ridge favorable for precipitation.

3. The vorticity distribution around a wind maximum in the jet stream similarly indicates areas of cyclonic relative vorticity advection and therefore potential precipitation.

Riehl [4] has developed a model for the distribution of vorticity around a wind maximum in the jet stream. Assuming no curvature, relative vorticity is a function only of the wind shear (cf. [5]). From figure 6 it is evident that the cyclonic wind shear is greatest to the north and the anticyclonic wind shear greatest to the south of the wind maximum, and both decrease upstream and downstream. Therefore, the flow is from greater to lesser cyclonic relative vorticity in quadrant 1 and from lesser to greater anticyclonic relative vorticity in quadrant 3. These quadrants thus have the requisite advection of cyclonic relative vorticity for upward vertical motion leading to precipitation. In quadrants 2 and 4 the advection is reversed and conditions are considered unfavorable for precipitation.

4. EFFECTS OF JET ON PRECIPITATION

In the lower troposphere conditions were extremely favorable for precipitation during the entire period under

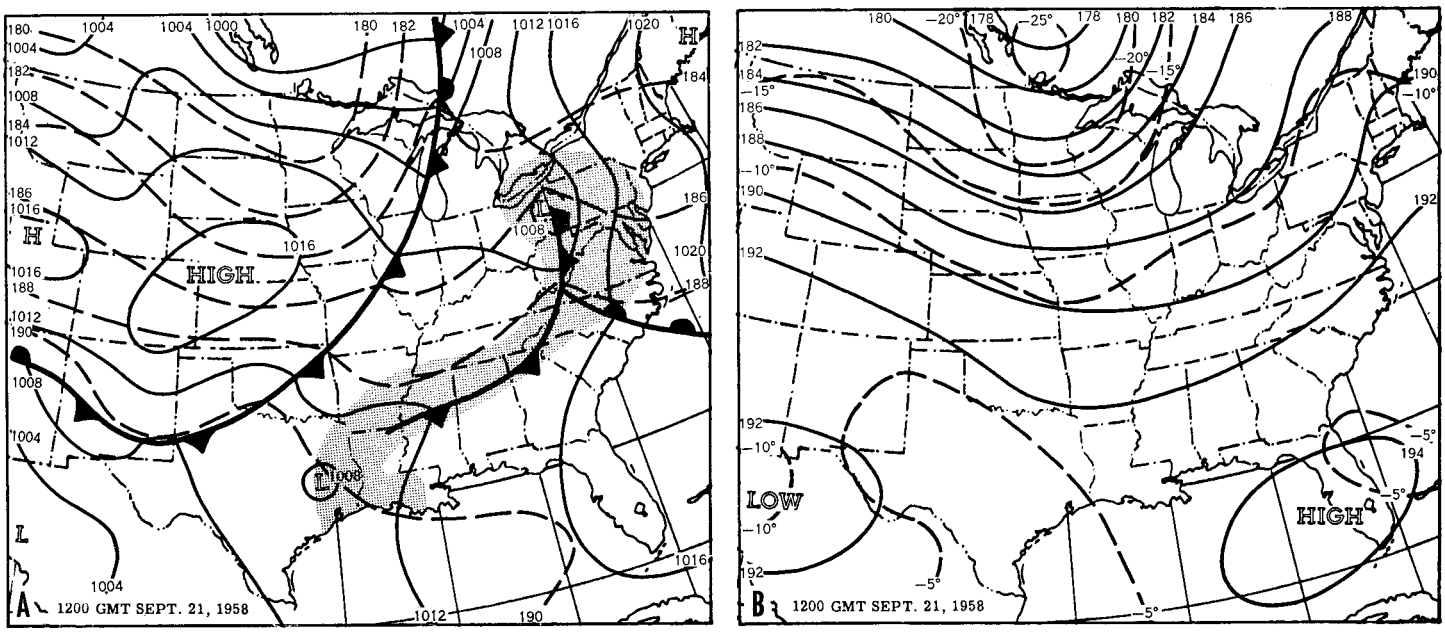

FIGURE 5.—Surface and 500-mb. charts for 1200 GMT, September 21, 1958.

study [6]. The moisture content of the atmosphere over the western Gulf States was near saturation (see fig. 9B) and the stability index chart (not shown) indicated the mT airmass was fairly unstable [7]. The low-level southerly flow from the Gulf of Mexico during the period had absorbed much moisture and was directed normal to the temperature gradient (note thickness lines on surface chart, fig. 1A), ensuring continuous warm air advection and low-level convergence in the western Gulf States.

At 1200 GMT, September 19 (fig. 7A), a jet with two distinct wind maxima extended from southern New Mexico through northern Tennessee to the Atlantic Coast near the North Carolina-South Carolina border. The position of the current rainfall over Arkansas, northern Louisiana, and northeastern Texas in relation to the definite wind maximum on the jet axis near Nashville, Tenn. could be described as being in quadrant 3 according to the scheme of figure 6; in figure 7A this quadrant is over a region where the surface isobars had no curvature. The active precipitation in central Texas was more difficult to associate with favorable high-level conditions. While the isotach analysis on the jet chart indicated another wind maximum, which incidentally remained generally near the New Mexico-Texas border throughout the entire 3-day period, it was considered to be in an unfavorable position (quadrant 4) for explaining that rainfall area.

The corresponding surface map (fig. 1A) shows weak cyclonic curvature of the isobars in southeastern Texas. As the air from the Gulf of Mexico moved over land, the increased friction caused the wind to blow across the isobars at a greater angle, thereby creating low-level convergence and upward vertical motion and thus abetting showers [8]. These tropical-like showers, which could have been enhanced by some undetected impulse of low-level vorticity advection from the remains of Gerda, were apparently not affected by conditions in the upper troposphere.

Twelve hours later, at 0000 GMT, September 20 (fig. 7B), the wind maximum, which was previously near Nashville, Tenn., had moved northward and wind speeds had increased. The intensity of the associated precipitation had increased as is shown by the superimposed 2-inch isohyet representing the latest 12-hour total amounts ending at the synoptic time.

Once again there was the problem of rationalizing the rains in eastern Texas because the jet chart again indicated decreasing anticyclonic shear downstream; i. e., unlikely conditions for precipitation. Observations of the sea level chart (fig. 2A), on the other hand, showed practically the same picture as the previous map with perhaps a slight increase in low-level convergence resulting from the formation of a weak Low near Waco, Tex.

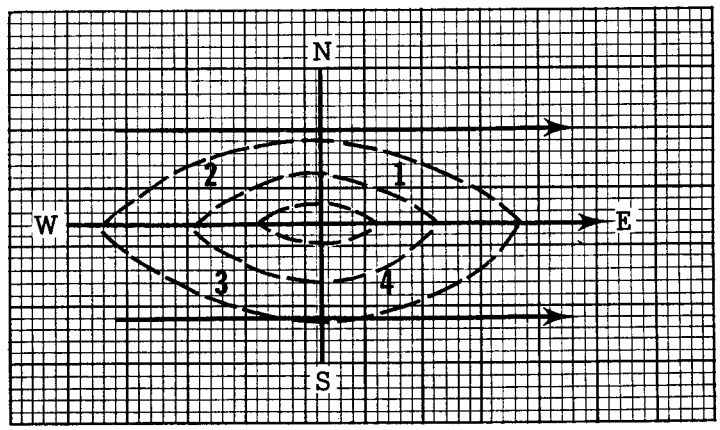

FIGURE 6.—Model for distribution of vorticity around a wind maximum in the jet stream. Streamlines (solid lines), isotachs (dashed lines).

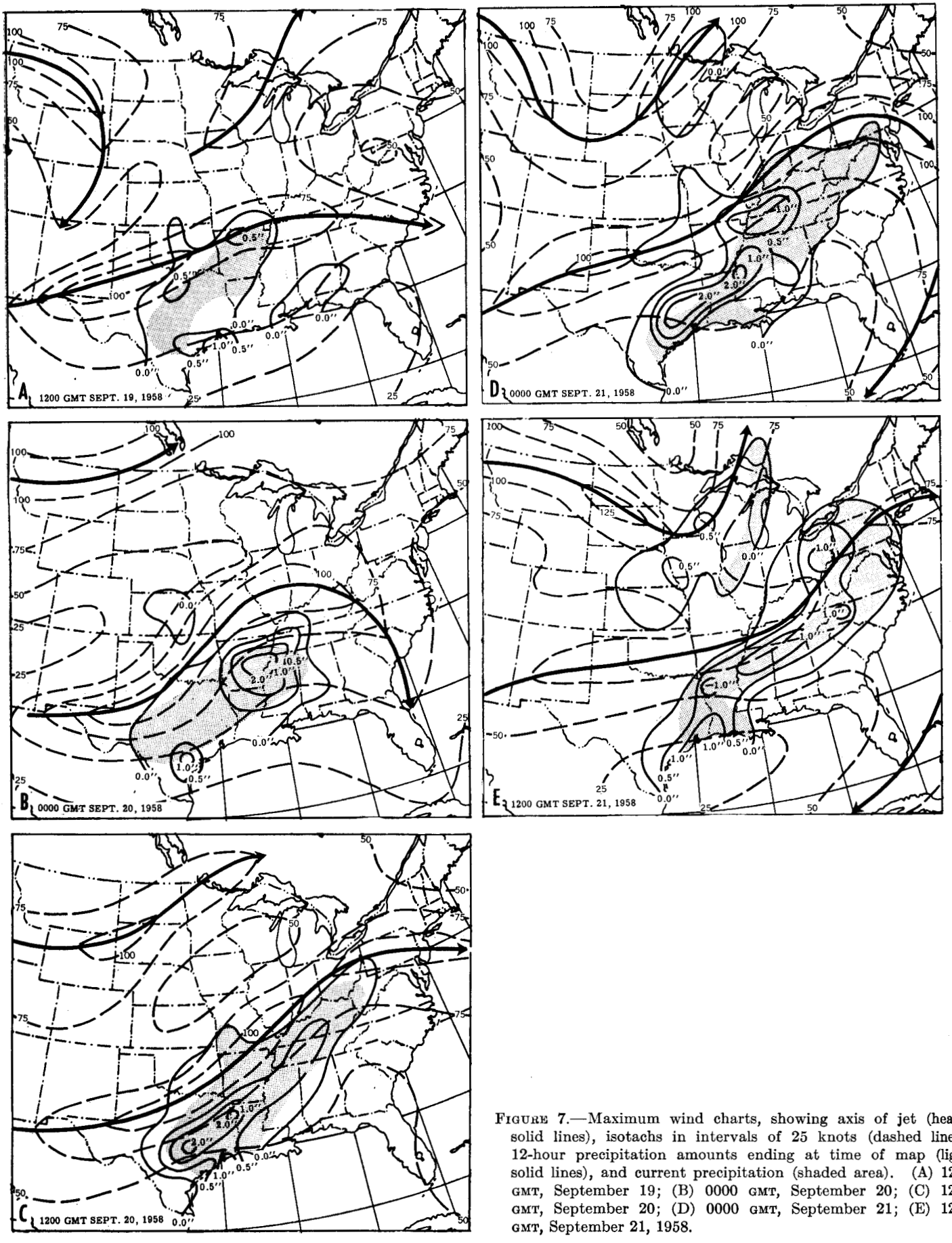

FIGURE 7.—Maximum wind charts, showing axis of jet (heavy solid lines), isotachs in intervals of 25 knots (dashed lines), 12-hour precipitation amounts ending at time of map (light solid lines), and current precipitation (shaded area). (A) 1200 GMT, September 19; (B) 0000 GMT, September 20; (C) 1200 GMT, September 20; (D) 0000 GMT, September 21; (E) 1200 GMT, September 21, 1958.

At 1200 GMT, September 20 (fig. 7C), the position of the jet and the maximum winds along it had moved farther northward to central Pennsylvania and the rain had spread into southern Ohio and western West Virginia. A second region of maximum winds was found over southeastern Missouri with its associated current precipitation and heavy 12-hour amounts over the Lower Mississippi Valley located in the favorable quadrant 3. (It is not the intention of the authors to discount completely any relationship whatsoever of the precipitation to the wind maximum in certain areas of the previous charts. But rather, there were no doubt several wind maxima running along the jet, and the lapse in time between observations and the distance between reporting rawin stations made detection of these oscillations nearly impossible [9].)

The corresponding surface chart (fig. 3A) now revealed cyclonic curvature in all of the isobars from the Low, which had moved northeastward to near Shreveport, La., to the high pressure ridge over the Atlantic coast.

At 0000 GMT, September 21 (fig. 7D), the previous two separate wind maxima consolidated into a single maximum located over eastern Pennsylvania-New Jersey. Again the precipitation belt was in quadrant 3, extending eastward to western Virginia, western Maryland, and southern Pennsylvania. The 1-inch isohyet over western Kentucky and western Tennessee, representing the area of heaviest 12-hour rainfall amounts, was also in that favorable position for nearly the entire half-day period. Of course it should be noted that the surface Low (fig. 4A), then located over western Kentucky with still a weak but definite closed circulation, moved directly over this rainfall area; the increased low-level convergence certainly increased the total precipitation. The rains in northern Mississippi and Louisiana, doubtless under the influence of the jet for a good part of the period, were interspersed with regions of thunderstorm activity, thus accounting for that precipitation maximum. Concurrently, a weak tropical depression had entered the southern Texas coast causing considerable rainfall and in turn, the third maximum 12-hour rainfall area in southeastern Texas.

During the next 12 hours, the precipitation spread northeastward to western New York and New Jersey (fig. 5A) in association with the now more pronounced Low over southwestern Pennsylvania. The corresponding jet map (fig. 7E), showed current rainfall amounts of any consequence to be north of the axis of highest winds for the first time. It must be remembered, however, that the surface system was by that time occluded, and the jet, which previously had been found exclusively north of the Low, was dropping southward. The jet eventually crossed the occluded front but still remained north of the warm and cold fronts, a usual occurrence according to Vederman's [10] idealized model relating the life cycle of extratropical cyclones to the jet. A second wind maximum over southern Kentucky accounted for the precipitation in Tennessee, northern Alabama, northern Mississippi, and southeastern Arkansas. Since the rainfall in Louisiana and eastern Texas was not associated with the jet, we refer to the surface chart (fig. 5A). The precipitation was caused by the abundant moisture and low-level convergence being propagated northeastward by the weak tropical Low located in eastern Texas.

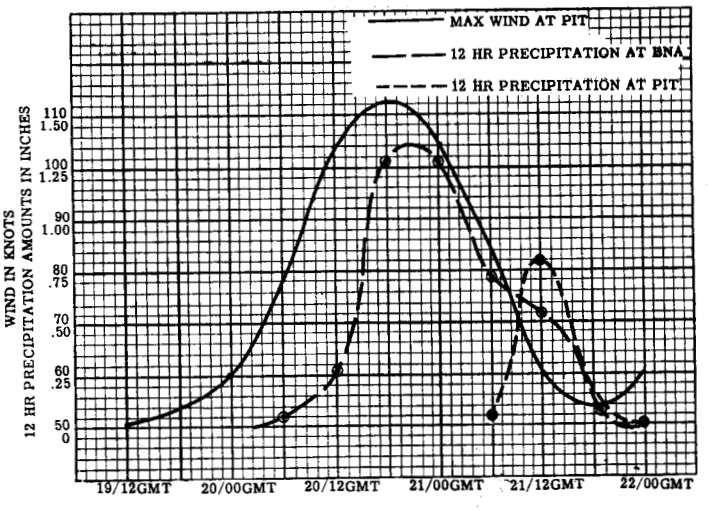

FIGURE 8.—Comparison of maximum wind profile at Pittsburgh with 12-hour accumulated precipitation at Nashville and Pittsburgh. (Precipitation plotted at end of 12-hour periods.)

At 0000 GMT, September 22 (chart not shown), as the sea level Low previously near Pittsburgh, Pa., was absorbed into the general circulation of the polar system to its west, the associated jets amalgamated over the northeastern United States. The southernmost jet then dissipated in the Central Mississippi Valley region and the precipitation over the Gulf States eventually tapered off to some scattered showers along the gulf coast itself.

Figure 8 illustrates the relationship with time of the jet maximum at Pittsburgh, Pa., to the 12-hour precipitation at Nashville, Tenn. The relationship is consistent with Riehl's quadrant 3 position as being a likely location for the heaviest amounts of precipitation to occur. Since Nashville is approximately 400 miles southwest of Pittsburgh, Nashville's 12-hour precipitation amounts reached a peak at nearly the same time as the wind in the jet core over Pittsburgh attained its highest speed; that is, the rainfall maximum lagged the jet maximum with time. This relationship can better be seen by noting the lag of about 18 hours between the wind maximum and the preciptiation maximum observed at Pittsburgh.

There was also a noticeable difference in the peak amounts of observed 12-hour rainfall at Nashville and Pittsburgh even though the available precipitable water over both of these cities was the same at their respective times. Comparison of figures 7D and 7E over the northeastern United States reveals a marked reduction in the speed of the wind maximum and also in the velocity gradient south of the jet in the 12-hour period. Thus the half-inch difference in peak precipitation totals could be attributed to the decrease in the gradient of wind shear and therefore of vorticity advection.

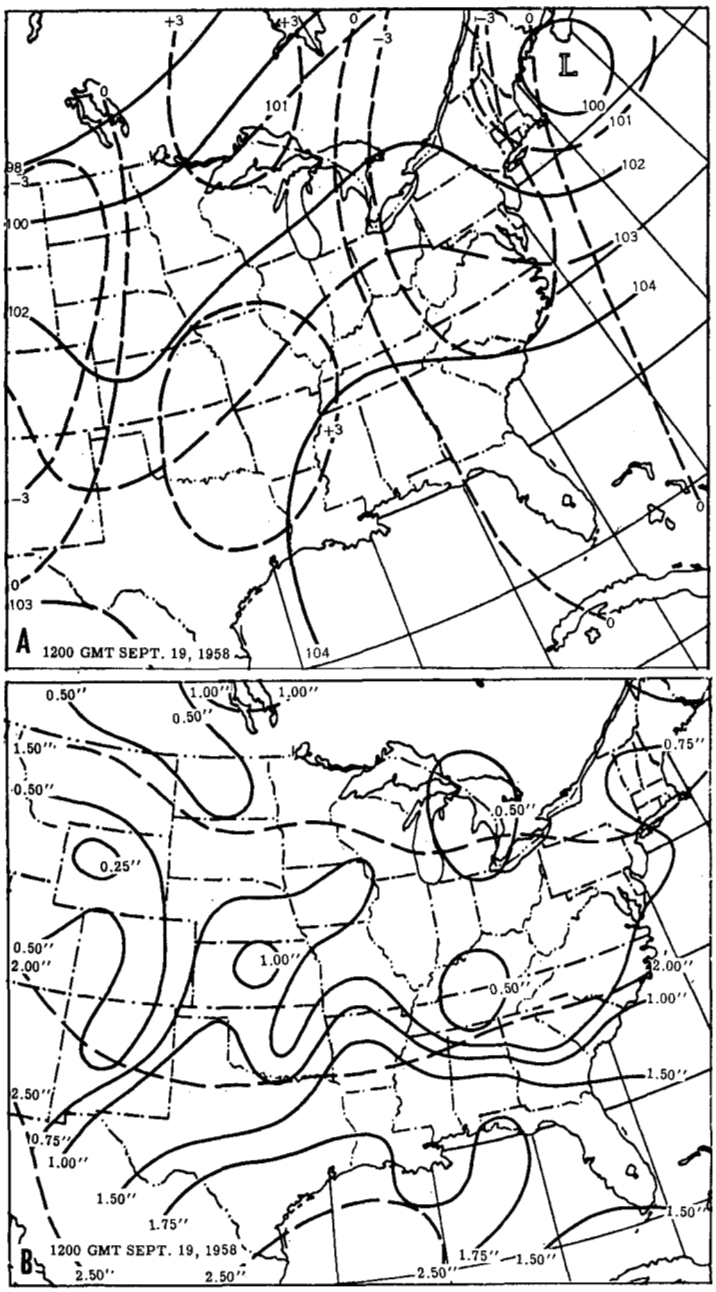

FIGURE 9.—1200 GMT, September 19, 1958. (A) 700-mb. chart, with contours (solid lines) in hundreds of geopotential feet, and vertical motion isolines (dashed) in millimeters per second. (B) Precipitable water chart. Available moisture isolines (solid) in inches. Saturation isolines (dashed) in inches.

5. TEST OF A METHOD OF FORECASTING 24-HOUR QUANTITATIVE PRECIPITATION

A procedure for forecasting quantitative precipitation, based mainly on surface considerations and requiring 3 hours to complete, was developed by the Hydrometeorological Section and tested by some of its members [1]. NAWAC has adopted a part of this procedure, namely, the relationship which exists among the expected area of precipitation, the inflow area, the available moisture, and the efficiency factor. The procedure below, while not presented as an improvement on the original method, incorporates some time-saving modifications that were necessary for the procedure to be operationally successful at NAWAC. These include the use of the initial and prognostic 700-mb. charts, the current and prognostic JNWP vertical motion charts, and the 1,000–500-mb. precipitable water chart. Consequently, the procedure as presented here involves the following parameters: (1) the area of expected 24-hour precipitation, A_p; (2) the area of 24-hour inflow at the 700-mb. level, A_i; (3) the 1,000–500-mb. mean available moisture, $\overline{W}$, over both the precipitation and inflow areas; and (4) the efficiency factor.

With minor refinements, the +3 mm./sec. vertical motion isoline was related to the area of expected precipitation. For example, on the initial vertical motion chart (fig. 9A) the area enclosed by the +3 mm./sec. isoline, minus that portion where a dry tongue of air extended southward over Oklahoma (fig. 9B), corresponded to the initial precipitation area (fig. 1A). The 24-hour precipitation area, A_p, then became the area swept out by the refined area enclosed by the +3 mm./sec. isoline on the initial vertical motion chart plus that area enclosed by the +3 mm./sec. isoline on the prognostic vertical motion chart. The 24-hour inflow area, A_i (fig. 10A), was determined by going upstream on the 700-mb. chart a calculated distance based on the expected 24-hour mean wind at the rear of A_p. For example, a 20-knot mean wind at the rear of A_p would correspond to an inflow area having a penetration of 480 nautical miles or 8 degrees of latitude into the airmass to the rear of A_p.

The dimensions of A_p and A_i are unimportant because all that is needed is a proportional relationship. In this situation a sheet of graph paper was placed over A_i and A_p and the squares covering each of these areas counted. The totals were 38 for A_p and 27 for A_i. Then, by placing the area represented by both A_p and A_i over the initial precipitable water chart an average value of the available moisture, $\overline{W}$, was computed to be 1.55 inches. Assuming that all of the available moisture will fall out, we apply the formula $\overline{W}(A_p+A_i)/A_p$ to obtain the average expected precipitation, which in this case was 2.65 inches per 24 hours. But, since we know from experience that not all of the available moisture does fall out, a highly subjective efficiency factor must be introduced. In this case an efficiency factor of 55 to 60 percent was suggested which reduced the 2.65-inch average over A_p to a more realistic 1.5 inches.

The efficiency factor is of critical importance to the success of this particular quantitative precipitation forecast method. Limited testing has indicated that the value of the efficiency factor should be near 50 percent most of the time, but may approach 100 percent for very small areas of expected precipitation which are located in and downstream from regions containing large amounts of available moisture. The efficiency factor drops off for large areas of expected precipitation, areas of low available moisture, and for airmasses with moisture concentration at high levels. The stability of the airmass must also

influence the efficiency factor, but this effect is unknown at this time.

The maximum precipitation area, P_m (fig. 10A) is defined as that portion of A_p enclosed by the isohyet of the average value. Recent studies at NAWAC concerning summertime-type precipitation areas suggest that the depth-distance curves should approximate the "normal" curve and that the mean isohyet should enclose the central one-fifth to one-sixth of the total precipitation area. Wintertime-type precipitation areas would logically have a more uniform precipitation distribution and, consequently, a larger centrally located P_m relative to the total precipitation area. Since the precipitation area under discussion was definitely a summertime-type, the 1.5-inch isohyet might be expected to enclose the central one-fifth to one-sixth portion of A_p. However, a refinement became apparent since the +3 mm./sec. vertical motion line enclosed part of the southwestern portion of A_p for the entire 24-hour period, and, for this reason, P_m was shifted toward the southwest from the geometric center.

The correlation of both A_p and P_m with precipitation which actually occurred (fig. 10B) was reasonably good, although both were displaced slightly to the east of the verification area. The error apparently developed because the +3 mm./sec. vertical motion isoline progressed more rapidly than did the higher available moisture values. Further refinements could make this forecast method more accurate, but time-consuming modifications would detract from its usefulness at NAWAC.

6. CONCLUSIONS

The authors do not intend to minimize the value of generally recognized tools for forecasting cloudiness, precipitation, and the movement and subsequent deepening of extratropical wave cyclones. We do feel, however, that there is much merit in using maximum wind forecasts along the jet as an additional means of arriving at regions of expected rainfall. Since there is a definite time lag between wind maxima and precipitation maxima at a given location, the problem becomes one of determining the approximate elapsed interval between the two maxima or of correlating the distance between the wind maximum at one station and the precipitation maximum at another.

The semi-objective quantitative precipitation forecast method presented in this article is based on limited testing, and quite certainly improvements of the subjective techniques advanced here will result from further usage. The immediate benefit from this method will be improved forecasting of the magnitude and the location of the 24-hour maximum precipitation area. At NAWAC established procedures for precipitation forecasting, especially in rain or no-rain situations with respect to time, will continue to be based primarily on the prognostic patterns of the respective surface and 500-mb. charts.

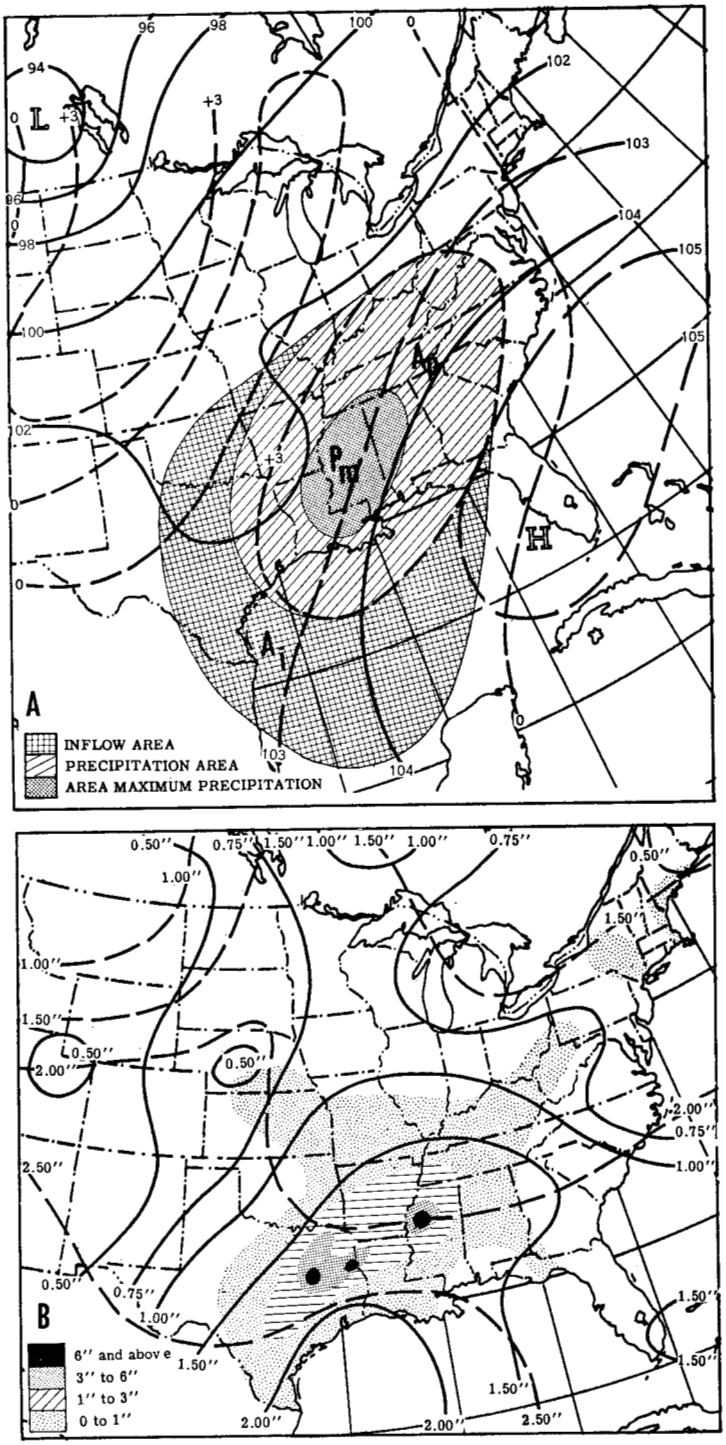

FIGURE 10.—1200 GMT, September 20, 1958. (A) 700-mb. chart with contours (solid lines) in hundreds of geopotential feet, Vertical motion isolines (dashed) in millimeters per second. A_p represents area of expected 24-hour precipitation ending at 1200 GMT, September 20. A_i represents area of expected 24-hour inflow ending at 1200 GMT, September 20. P_m shows area of expected maximum 24-hour rainfall ending at 1200 GMT September 20, 1958. (B) Precipitable water chart. Available moisture isolines (solid). Saturation isolines (dashed). Isohyetal lines represent 24-hour precipitation amounts ending at 1200 GMT, September 20, 1958.

ACKNOWLEDGMENTS

The writers express their appreciation to staff members of NAWAC for helpful suggestions and critical review of this article, to members of JNWP Unit for their cooperation, and to the Daily Map Unit of the Weather Bureau for drafting of the figures.

REFERENCES

1. C. S. Gilman, H. V. Goodyear, and K. R. Peterson, On Quantitative Precipitation Forecasting, Hydrometeorological Section, U. S. Weather Bureau, Washington, 1958 (Unpublished manuscript).
2. U. S. Weather Bureau, *Tropical Storm Gerda, September 13–15, 1958, A Preliminary Report and the Advisories Issued,* Sept. 30, 1958.
3. H. Riehl, K. S. Norquest, and A. L. Sugg, "A Quantitative Method for the Prediction of Rainfall Patterns," *Journal of Meteorology,* vol. 9, No. 5, Oct. 1952, pp. 291–298.
4. H. Riehl et al., "The Jet Stream," *Meteorological Monographs,* vol. 2, No. 7, American Meteorological Society, August 1954, 100 pp.
5. H. Panofsky, *Introduction to Dynamic Meteorology,* The Pennsylvania State University, University Park, Pa., 1956, 243 pp.
6. S. Teweles, Jr., "A Test of the Relation Between Precipitation and Synoptic Patterns at 200 and 300 Millibars," *Journal of Meteorology,* vol. 10, No. 6, Dec. 1953, pp. 450–456.
7. V. J. Oliver and R. F. Shaw, "Heavy Warm-Sector Rains from Illinois to the Middle Atlantic Coast, May 26–28, 1956," *Monthly Weather Review,* vol. 84, No. 5, May 1956, pp. 198–204.
8. S. Petterssen, *Weather Analysis and Forecasting,* vol. II, McGraw-Hill Book Co., Inc., New York, 1956.
9. J. Badner and M. A. Johnson, "Relationship of Tropopause and Jet Streams to Rainfall in Southeastern United States, February 4–9, 1957," *Monthly Weather Review,* vol. 85, No. 2, Feb. 1957, pp. 62–68.
10. J. Vederman, "The Life Cycles of Jet Streams and Extratropical Cyclones," *Bulletin of the American Meteorological Society,* vol. 35, No. 6, June 1954, pp. 239–244.

U. S. GOVERNMENT PRINTING OFFICE: 1958